

Local density of states of a d -wave superconductor with inhomogeneous antiferromagnetic correlations

W. A. Atkinson
Trent University

(Dated: November 20, 2018)

The tunneling spectrum of an inhomogeneously doped extended Hubbard model is calculated at the mean field level. Self-consistent solutions admit both superconducting and antiferromagnetic order, which coexist inhomogeneously because of spatial randomness in the doping. The calculations find that, as a function of doping, there is a continuous cross over from a disordered “pinned smectic” state to a relatively homogeneous d -wave state with pockets of antiferromagnetic order. The density of states has a robust d -wave gap, and increasing antiferromagnetic correlations lead to a suppression of the coherence peaks. The spectra of isolated nanoscale antiferromagnetic domains are studied in detail, and are found to be very different from those of macroscopic antiferromagnets. Although no single set of model parameters reproduces all details of the experimental spectrum in $\text{Bi}_2\text{Sr}_2\text{CaCu}_2\text{O}_8$, many features, notably the collapse of the coherence peaks and the occurrence of a low-energy shoulder in the local spectrum, occur naturally in these calculations.

I. INTRODUCTION

Nanoscale inhomogeneities have been widely observed in the high temperature superconductor (HTS) $\text{Bi}_2\text{Sr}_2\text{CaCu}_2\text{O}_8$ (BSCCO), primarily through scanning tunneling microscopy (STM) experiments performed in the superconducting state.^{1,2,3,4,5,6,7} At present, the origins of the inhomogeneity are not well understood, although it is very plausible that they are directly correlated with variations in the local doping concentration. In BSCCO, the hole concentration is controlled by the addition of interstitial oxygen atoms which appear to reside ≈ 5 Å above the conducting CuO_2 layers. Because of the short distance, large spatial fluctuations of the Coulomb potential are expected in the CuO_2 layers, especially in underdoped samples where screening is poor. In STM experiments (which do not measure local doping directly), nanoscale inhomogeneities are manifested most strongly in the magnitude Δ_T of the superconducting gap in the tunneling spectrum. Interestingly, regions with small Δ_T exhibit large coherence peaks at the gap edge, while the coherence peaks are essentially missing in regions with $\Delta_T > 65$ meV. These latter regions are assumed to represent an underdoped “pseudogap” phase which may be quite distinct from the small-gap “superconducting” (SC) regions. Though speculative, this labelling is supported by the fact that the “pseudogap” regions occupy a large fraction of the strongly underdoped samples, and relatively little of the optimally doped samples.⁷

The simplest model of the inhomogeneities is that the pairing energy depends strongly on doping,^{8,9,10} with the “pseudogap” domains corresponding to regions of large pairing energy which are nonsuperconducting because of phase fluctuations. It is also possible that secondary phases may coexist with the SC state, forming spontaneously, or perhaps being nucleated in hole-poor domains. Theoretical calculations from the early days of high-temperature superconductivity^{11,12,13,14} suggest the possibility of self-organized stripe formation, and in some materials (notably $\text{La}_{2-x-y}\text{Nd}_y\text{Sr}_x\text{CuO}_4$ ¹⁵) there is solid

evidence for stripes, though it has generally been hard to substantiate in other materials. A large variety of other competing or coexisting phases have been discussed since the discovery of HTS, and the list includes charge density wave (CDW),^{16,17} spin Peierls,^{18,19} antiferromagnetic or spin density wave,^{20,21,22,23} pair density wave,^{17,24} staggered flux²⁵, and orbital current^{18,26,27,28} phases.

Experimentally, optimally-doped BSCCO^{29,30,31} appears to support a fairly straightforward d -wave BCS picture of superconductivity rather well,^{31,32,33,34,35} although similar experiments^{5,6} have been interpreted in terms of commensurate stripe formation with a periodicity of $\approx 4a_0$ where $a_0 \approx 5$ Å is the lattice constant. At lower doping, other recent work⁷ finds weak “checkerboard” charge modulations with a periodicity close to that measured in Refs. [5,6], with the weight of the modulations being reduced as the doping increases. However, the situation is not transparent since the modulations are only seen at energies larger than the gap edge (contrary to what one might expect in a stripe scenario), are only seen in the “pseudogap” regions, and the modulation wavelength is comparable to the typical size of the “pseudogap” domains. There is a further ambiguity in determining what, if any, ordering is present: many ordered phases (eg. antiferromagnetism) which may be relevant to BSCCO couple weakly to the local charge density and are not easily identified in STM experiments. Thus, it is not clear whether the weak charge modulations seen in experiments are the dominant ordering, or whether they are secondary manifestations of some hidden order. For these reasons, it may be difficult to detect and study coexisting order based on spatial modulations of the local density of states (LDOS) alone.

The goal of the present work is to look for signatures of inhomogeneously coexisting order in the energy dependence of the local spectrum. For definiteness, I adopt a model in which antiferromagnetic (AF) correlations compete with SC order. From a calculational perspective, this is the simplest and least ambiguous choice, although other order parameters—particularly CDW order

(including checkerboard order)—are also potentially relevant to the STM experiments cited above. Many of the results of this paper will actually apply broadly to other forms of competing order, and I will try distinguish these results from those which are specific to antiferromagnetism. Having said this, I want to remark that antiferromagnetism is a natural choice to make given the proximity of the AF and SC phases in the HTS phase diagram, and that other authors have studied similar models.^{12,20,21,23} In addition, there is mounting evidence that glassy (short-ranged) quasistatic AF correlations are significant in underdoped HTS,^{36,37,38,39,40,41} including BSCCO,⁴¹ and it is important to understand how these correlations are manifested in the LDOS.

The paper is organized as follows: In Sec. II A, I introduce the model, and perform calculations for a finite-sized, inhomogeneously doped d -wave superconductor with competing AF and SC order. Short range AF order arises naturally in the current work because the system is doped inhomogeneously by charged out-of-plane donors and AF moments form preferentially in underdoped regions. At low doping levels, I find that the self-consistently determined electronic state resembles a “pinned smectic” in which superconductivity is pronounced along domain walls of the AF background. At higher doping, there is a crossover to a fairly homogeneous d -wave SC state with occasional pockets of AF order. In all cases, there is a well defined d -wave gap in the spectrum. Since the spectral energy resolution suffers from finite-size effects, I discuss the LDOS in the context of a single underdoped pocket embedded in a homogeneous d -wave superconductor in Sec. II B. Several spectral features measured in [7], notably the suppression of coherence peaks, the appearance of shoulders in the spectrum, and the homogeneity of the low energy spectrum, can be understood in these calculations, although no single parameter set reproduces simultaneously all the experimentally measured spectral features. One of the most important conclusions of this section is that, because of the nonlocality of quasiparticles, the local spectrum of an AF pocket resembles neither that of macroscopic antiferromagnets or superconductors (nor is it an average of the two): The introduction of inhomogeneity on the nanometer length scales leads to a qualitatively new spectrum. This is a significant finding since one of the main arguments against coexisting secondary phases is that, apart from the special case of a nested Fermi surface, any *macroscopic* ordering which is commensurate with the lattice has a spectrum which is not particle-hole symmetric, in contradiction with experiments. I find, however, that inhomogeneous ordering on nanometer length scales *may*, in fact, yield a particle-hole symmetric spectrum. These calculations are interpreted in terms of a three-band model of homogeneously coexisting SC and AF order in Sec. II C. The issue of how charge modulations arise in this model is discussed in Sec. II D. Conclusions are presented in Sec. III.

II. CALCULATIONS AND RESULTS

A. Inhomogeneously doped superconductor

The basic Hamiltonian is the Hubbard model with a long-range Coulomb interaction and SC pairing interaction:

$$\begin{aligned}
 H = & \sum_{i,j,\sigma} t_{ij} c_{i\sigma}^\dagger c_{j\sigma} - Z \sum_{i,\mathbf{R}} V(\mathbf{r}_i - \mathbf{R}) \hat{n}_i \\
 & + \sum_i U \hat{n}_{i\uparrow} \hat{n}_{i\downarrow} + \frac{1}{2} \sum_{i \neq j} V(\mathbf{r}_i - \mathbf{r}_j) \hat{n}_i \hat{n}_j \\
 & + \sum_{ij} \Delta_{ij} (c_{i\uparrow}^\dagger c_{j\downarrow}^\dagger + c_{i\downarrow} c_{j\uparrow}) \quad (1)
 \end{aligned}$$

where $c_{j\sigma}$ is the spin- σ annihilation operator at site j , $\hat{n}_{i\sigma}$ and \hat{n}_i are the spin-resolved and total charge density operators at site i , and \mathbf{r}_i is the position of the i^{th} site. I use a third-nearest neighbor conduction band with parameters t_0, \dots, t_3 describing the on-site potential, nearest, next-nearest, and third-nearest neighbor hopping amplitudes. Throughout this work, all energies are given in units of $|t_1|$ which (for reference) is $\sim O(100)$ meV. I take $\{t_1, t_2, t_3\} = \{-1, 0.25, -0.1\}$ and adjust t_0 to give the desired filling. The long range Coulomb interaction is $V(\mathbf{r}) = (e^2/\epsilon a_0)|\mathbf{r}|^{-1}$ where \mathbf{r} is measured in units of the lattice constant a_0 , $e^2/\epsilon a_0 = 1$, and the on-site interaction is absorbed into the Hubbard U term: $V(0) = U/2$. The impurities are located at positions \mathbf{R} , which sit a distance $d_z = 1.5a_0$ above randomly chosen lattice sites. The final term in the Hamiltonian is added as an ansatz to describe SC order arising from spin-interactions between neighboring sites. The local bond order parameter $\Delta_{ij} = -\frac{J}{2} \langle c_{j\downarrow} c_{i\uparrow} + c_{j\uparrow} c_{i\downarrow} \rangle$ is determined self-consistently for nearest neighbor sites i and j . The Coulomb interaction is treated in the Hartree approximation, and the effective mean-field Hamiltonian can be diagonalized numerically to extract eigenstate wavefunctions and the corresponding eigenenergies. The fields Δ_{ij} and $n_{i\sigma}$ are iterated to self-consistency on small lattices with between 20×20 and 40×40 sites. The calculations are unconstrained, and are seeded with a finite antiferromagnetic moment. In order to improve convergence, which is problematic when magnetic moments form, a combination of Thomas-Fermi and Pulay method charge-mixing is used at each iterative step.⁴²

Figure 1 shows typical results for an underdoped superconductor for the self-consistent hole density $n_{hi} = 1 - n_i$ with $n_i = \langle \hat{n}_i \rangle$, the staggered AF moment $m_i = \frac{1}{2} e^{i\mathbf{Q} \cdot \mathbf{r}_i} (n_{i\uparrow} - n_{i\downarrow})$ with $\mathbf{Q} = (\pi, \pi)$, and the d -wave order parameter $\Delta_i^{(d)} = \frac{1}{2} \sum_{\delta} (-1)^{\delta_y} \Delta_{i+i\delta}$ where δ is summed over the four nearest-neighbor sites. The average hole density is $n_h \equiv 1 - n \approx 0.07$ holes/site, but the hole distribution is quite inhomogeneous. In a homogeneously doped sample with $J = 1.5$ and $U = 3.2$ (these are typical for this work), there is a first order phase transition between SC and AF phases at a hole doping level

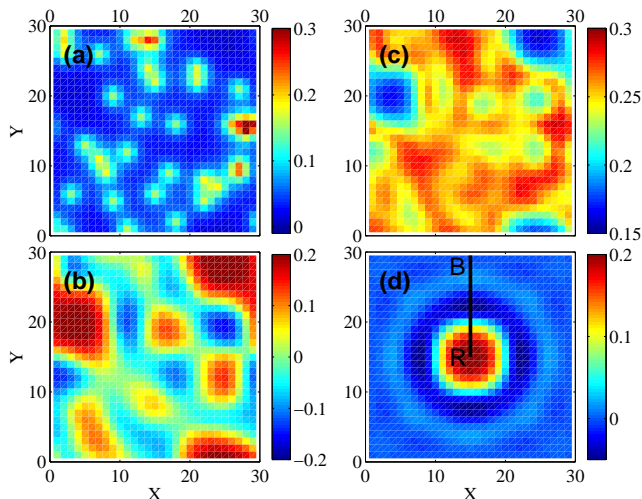


FIG. 1: Self-consistent solutions of the model. (a) Charge density, (b) staggered magnetization, and (c) d -wave gap are shown for a 30×30 lattice with 35 donor impurities of charge $Z = -2e$. The model parameters are $U = 3.2$ and $J = 1.5$. The corresponding hole doping level is $n_h \approx 0.07$. The staggered magnetization for a single underdoped disk of radius $4a_0$ is shown in (d). Notice that a small incommensurate moment is induced outside the underdoped disk. The LDOS along the line from R to B is shown in Fig. 3.

$n_h = 0.07$. In the inhomogeneous system, the situation is more complicated. The spin polarization saturates near its bulk value in undoped regions whose diameter exceeds $\xi_{AF} \sim t_1/U m$, where m is the staggered moment. In smaller underdoped regions, the staggered moment is roughly proportional to the diameter of the region. It is worth stressing that this behavior is very different from single-phase models in which the magnitude of the local order parameter is directly correlated with the local charge density,⁹ regardless of the size of the domain. Note also that, although the doped and undoped regions in Fig. 1 lie firmly on either side of the first order phase transition separating AF and SC phases, both order parameters are finite throughout the system because of a pronounced proximity effect. In this sense, the introduction of disorder in the doping leads to a qualitative change in the phase diagram. This aspect of the calculations appears to be consistent with neutron scattering studies in LSCO⁴⁰ suggesting that AF and SC coexist locally. One factor which appears inconsistent with experiment is that the d -wave order parameter is suppressed by static AF correlations, whereas there is good evidence that it actually grows rapidly as the insulating phase is approached in HTS. This disparity may be the result of the simplicity of the current mean-field approximation. In a more sophisticated treatment, the suppression of SC order will be compensated to some extent by the fact that the pairing interaction is doping dependent: Numerical studies of the t - J model^{8,10} find that $J \sim (1 + n_h)^{-2}$. Since this result was originally derived for homogeneous

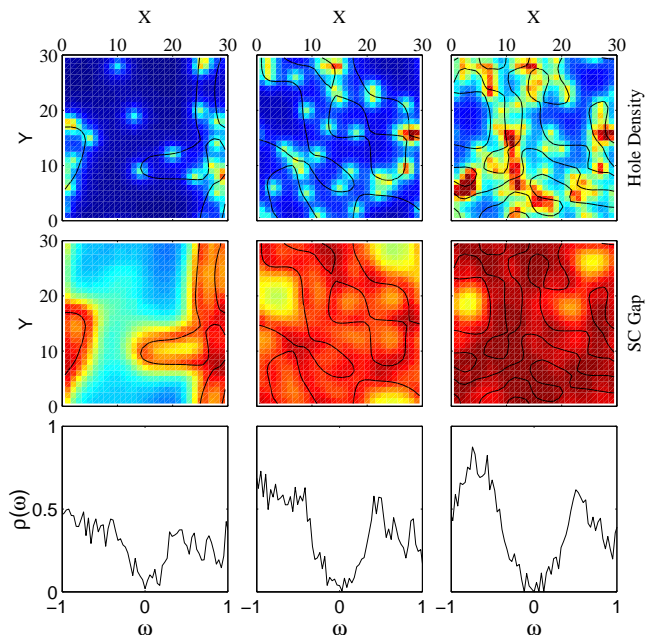


FIG. 2: Doping dependence of the AF and SC phases. The three rows display the hole density (top), SC gap (middle) and average density of states (bottom) for three different donor-impurity concentrations. The columns correspond to 20 donor-atoms (left), 35 donor-atoms (middle) and 70 donor-atoms (right). Contours show the domain walls of the staggered AF moments. Parameters are as in Fig. 1. The color scales are identical for all panels within a row, and are the same as in Fig. 1(a) and (c).

systems, and cannot be trivially extended to inhomogeneous systems (but should not change our conclusions qualitatively), I will defer its discussion rather than introduce an *ad hoc* local renormalisation of J .

Figure 2 shows how the coexisting phases evolve with hole doping. At low doping, the situation qualitatively resembles a pinned smectic. Smectic phases have been proposed as a natural mechanism by which doped antiferromagnets can accommodate holes while minimizing both the hole kinetic, antiferromagnetic exchange, and long range Coulomb energies.⁴³ Consistent with the smectic picture, the AF moments in Fig. 2 spontaneously form π -shifted domains whose boundaries are pinned to donor-impurity locations, and the SC order parameter $\Delta_i^{(d)}$ is largest along the domain walls. However, there are a number of differences between the current “weak coupling” mean-field calculations and the canonical “strong-coupling” smectic picture. First, because of frustration introduced by next-nearest neighbor hopping, the AF phase is never fully polarized. This same frustration leads to a gapless quasiparticle spectrum in the pure AF phase provided U is less than some model-dependent critical value. As a consequence, holes are not confined to domain walls but are mobile throughout the volume of the sample. In other words, although there are static AF cor-

relations, the system is on the metallic side of the metal-insulator transition. A further consequence, which distinguishes weak and strong-coupling approaches, is that the SC order parameter remains finite everywhere in the weak-coupling calculations.

As hole doping increases, the AF phase is suppressed through a proliferation of domain walls. In Fig. 2, significant AF moments form at higher doping only in regions where, due to randomness in the donor-atom distribution, undoped regions have diameters larger than ξ_{AF} . The system is then better understood as consisting of isolated AF pockets embedded in a relatively homogeneous d -wave superconductor. In this model, annealing (which tends to homogenize the charge distribution) will have significant effect on the extent of AF order.

Figure 2 also shows the spatially averaged density of states $\rho(\omega)$ for each of the disorder configurations. Although the data is noisy, several clear features are evident: First, as one underdopes, there is a gradual suppression of spectral weight on an energy scale which is large relative to the SC gap. Second, there is a robust d -wave gap, even in situations where a large fraction of the sample is antiferromagnetic. I emphasize that this latter effect is not necessarily anticipated since, in the absence of a nested Fermi surface, AF ordering tends to destroy the particle-hole symmetry of the spectrum. Third, as one underdopes, the superconducting coherence peaks are suppressed. As discussed in the introduction, the suppression of coherence peaks is one of the hallmarks of the pseudogap phase of the underdoped cuprates. To my knowledge, this is the first reproduction of such an effect in terms of a static mean field model.

These results are rather encouraging and, ideally, the next step should be a detailed examination of the LDOS. However, finite size effects limit the spectral resolution to the extent that the LDOS is impossible to interpret. Consequently, I will focus for the remainder of the paper on intermediate doping levels where one can improve the energy resolution by studying isolated underdoped pockets embedded in a large superconducting domain. A more detailed exploration of the pinned smectic phase requires a different approach and is, unfortunately, beyond the scope of this work.

B. Single underdoped pocket

It is difficult to discuss the STM spectrum in detail for finite-sized lattices because of the discreteness of the spectrum. For a 30×30 lattice, one might typically have ≈ 100 subgap states, with the resulting spectrum being too noisy for anything other than the grossest analysis. I therefore study a single, isolated, AF pocket which is embedded in a homogeneous background potential corresponding to a hole doping level of $p \approx 0.15$ (in fact, the hole doping level is less important than the Fermi surface shape, and should not be taken too seriously). In this calculation, a positively charged disk of radius R

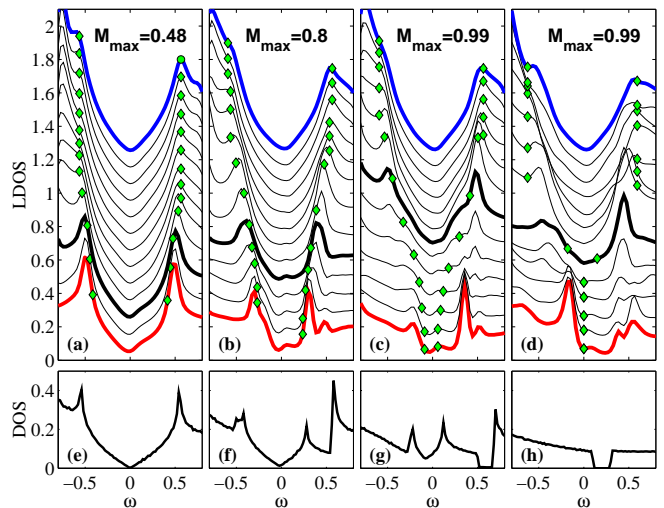


FIG. 3: Local density of states. (a)-(d) The LDOS is shown for different model parameters. The spectra, offset for clarity, are taken at a sequence of sites extending radially outwards along the (010) direction from the center of an isolated underdoped disk of radius R . The path along which spectra are measured is shown in Fig. 1(d), with points B and R corresponding to the blue (top) and red (bottom) curves in this figure. The heavy black curve in each panel indicates the site at which the staggered magnetization falls to half the maximum value m_{max} . Diamond symbols indicate $\pm 2\Delta_i^{(d)}$ (the estimated coherence peak energies) at each site. The first three panels are for (a) $U = 3.2$, $R = 1.5a_0$, (b) $U = 3.2$, $R = 4.0a_0$, and (c) $U = 3.4$, $R = 4.0a_0$. $J = 1.5$ throughout. In (d), spectra are calculated for a non-self-consistent model of a pure antiferromagnetic pocket of radius $R = 6.0$ with $U = 3.4$ embedded in a pure d -wave superconductor. The heavy black curve marks the sharp boundary between the AF and SC domains. For comparison, the DOS for homogeneously coexisting AF and SC order are shown in (e)-(h). Cases are (e) $(M, \Delta^{(d)}) = (0, 0.3)$, (f) $(0.3, 0.3)$, (g) $(0.6, 0.3)$, (h) $(1.0, 0)$.

sits $d_z = 1.5a_0$ above the conducting layer. The charge on the disk is adjusted so that the site under the center is half-filled. The charge, magnetization and SC gap are calculated self-consistently, and an example of the self-consistent magnetization for a disk of radius $R = 4a_0$ is shown in Fig. 1(d). In order to obtain a high spectral resolution, the underdoped pocket is embedded in a homogeneous 200×200 region and a recursion technique⁴⁴ is used to calculate $\rho(\mathbf{r}, \omega)$. In this way, I avoid spurious structures associated with the discreteness of the spectrum on finite lattices. Figure 3 shows the LDOS along cuts through the centre of an AF pocket for different values of $\{U, R\}$.

The spectra in Fig. 3 show a smooth evolution from regions where the d -wave order parameter is dominant, to the central region where AF correlations are large. The particle-hole asymmetry at large energies comes from a van Hove singularity at $\omega \approx -0.5|t_1|$. At lower energies, the spectrum is determined by the interplay between SC

and AF order. There are several noteworthy features of this calculation. First, there is an overall suppression of spectral weight at site i on an energy scale $M_i = Um_i$. For a nested Fermi surface, with homogeneous magnetization, M_i is the energy of the AF gap, but in the absence of nesting, AF correlations lead to a shift of states away from the Fermi level even when a true gap does not open. This shift is a precursor to the formation of lower and upper Hubbard bands, and is consistent with the observation of spectral weight shifts on a large energy scale as a function of doping in the cuprates. Two factors tend to suppress the nucleated moment: the frustration introduced by the next-nearest neighbor hopping (ie. the absence of complete nesting of the Fermi surfaces), and the competition with the superconducting phase. I want to emphasize a consequence of this which may not be intuitive: Although a large U may not generate a substantial moment m , the energy scale M over which the quasiparticle spectrum is affected by magnetic correlations can still be quite large. This is likely to be a universal feature of models of competing order in the cuprates. One could similarly imagine that, in a model with a charge ordered phase, frustration due to imperfect Fermi surface nesting and competition with SC order would tend to suppress the magnitude of charge modulations but still affect the spectrum over a relatively large energy scale.

A second feature of Fig. 3 is that the local dispersion in the AF pocket near the Fermi level is quasilinear when $M_i \lesssim \Delta_i^{(d)}$ [Fig. 3(a)]. This is a significant result since one of the main arguments against coexisting commensurate order in the cuprates is the absence of a linear dispersion at the Fermi level. When $M_i \gtrsim \Delta^{(d)}$, the LDOS becomes particle-hole asymmetric: as M_i increases (either as one moves into the AF pocket, or as one turns up U), a shoulder develops in the dispersion at low energies, which ultimately evolves into a well-defined resonance [Fig. 3(b)]. The energy of the resonance depends on the details of the band structure, and on $\Delta^{(d)}$, but is a universal feature in nearly all numerical results.

One of the most interesting aspects of Fig. 3 is the evolution of the coherence peaks between the SC and AF regions. There are actually two qualitatively different ways in which this occurs. In Figs. 3(a) and (b), the coherence peaks shift to lower energies, sharpen, and lose spectral weight as one moves into the AF domain. The coherence peak positions approximately reflect the local value of $\Delta^{(d)}$, which is what one might naively expect for a smoothly varying Hamiltonian. The situation is different in Fig. 3(c) where the magnetization is larger: the coherence peaks (starting at a point exterior to the AF domain and moving inwards) rapidly collapse, but shift rather little. The absence of a shift indicates that one is seeing the decaying tails of bulk BCS-like states. In other words, antinodal quasiparticles from the SC domain *tunnel* (rather than propagate freely) into the AF domain, and decay over some characteristic distance which determines the extent of the coherence peaks into the AF domain. I will argue below that this arises from a mis-

match in the SC and AF energy dispersions: when M is sufficiently large, the states at the antinodal k -vector are gapped in the AF domain.

The fact that the coherence peaks sharpen as one moves into the AF region in Fig. 3(a) and (b) is the result of the fact that the Fermi surfaces nest at isolated points (the contours $\epsilon_{\mathbf{k}} = 0$ and $\epsilon_{\mathbf{k}+\mathbf{Q}} = 0$ shown in Fig. 4 intersect at two points). Because of this peculiar nesting, spectral weight is removed at energies both above and below the antinodal saddle point energy (the point which generates the coherence peaks) by the AF correlations, but the saddle point itself survives until the AF moment becomes very large. Thus, the coherence peaks lose weight by narrowing rather than by being suppressed. Other competing phases (such as charge density waves) which nest differently should have a qualitatively different effect on the coherence peaks.

One surprising aspect of Fig. 3(b) and (c) is that although the transition from SC to AF domains occurs differently depending on the magnetization, the spectrum at the core of the AF pocket is quite similar. For comparison, a non-self-consistent calculation is shown in Fig. 3(d) for the ansatz

$$\Delta_{ij} = \begin{cases} 0, & |\mathbf{r}_i| < R \text{ or } |\mathbf{r}_j| < R \\ 0.3, & \text{otherwise} \end{cases},$$

$$m_i = \begin{cases} 0.3, & |\mathbf{r}_i| < R \\ 0, & \text{otherwise} \end{cases},$$

with $R = 6a_0$. Again, the spectrum at the core of the AF disk is quite similar to that of the self-consistent calculations shown in Fig. 3(b) and (c). (note the similarity in the peak positions), but bears little resemblance to the spectrum of the macroscopic AF phase shown in Fig. 3(h). This calculation demonstrates that the boundary conditions (the coupling between the AF pocket and the SC bulk) have as large an impact on the local spectrum at the core of the AF pocket as the local value of the SC order parameter. This is a central result: when the scale of the inhomogeneity is atomic, one cannot assume a direct correspondence between the local ordering and the local spectrum. In the following section, I argue that a qualitative understanding of the inhomogeneously doped system can be developed from a model of *homogeneously* coexisting SC and AF order.

C. Homogeneously coexisting order

I consider a three-band model of a homogeneous system with coexisting SC and AF long range order. The SC order parameter has the usual form $\Delta_{\mathbf{k}} = \Delta^{(d)}(\cos k_x - \cos k_y)$ and the AF order parameter is M with $m_i = M/U$. I adopt the same dispersion as before, with $\epsilon_{\mathbf{k}} = t_0 + 2t_1(\cos k_x + \cos k_y) + 4t_2 \cos k_x \cos k_y + 2t_3(\cos 2k_x + \cos 2k_y)$ and $t_0 = 0.7|t_1|$. For a complex frequency

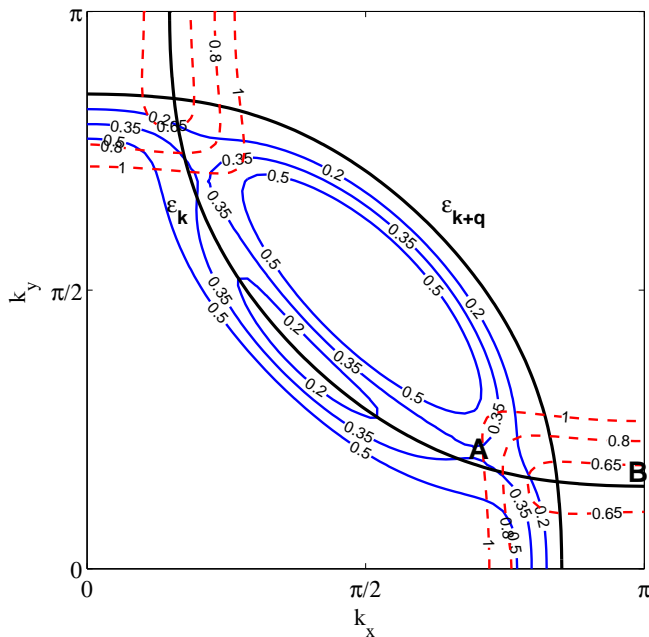


FIG. 4: Constant energy contours of the coexisting AF/SC model. Parameters are the same as Fig. 3(e). A few contours are shown for positive energies for the upper (dashed red) and middle (solid blue) bands. The zero-energy contours of $\epsilon_{\mathbf{k}}$ and $\epsilon_{\mathbf{k}+\mathbf{q}}$ are shown for reference. For small energies, the contours have the “banana”-like shape expected for d -wave superconductors, as well as an antiferromagnetic shadow band. There is a saddle-point singularity at $\omega = 0.38$ (labelled “A” in the figure) which marks the end of the linear dispersion, and gives rise to the $\omega = 0.38$ van Hove singularity in Fig. 3(f). There is a second saddle-point at B in the figure, which gives rise to the superconducting coherence peaks. The energies of the saddle-points depend on both $\Delta^{(d)}$ and M . For sufficiently large M , the saddle-point at B evolves into a simple band minimum, corresponding to the lower edge of the upper Hubbard band.

$z = \omega + i0^+$, the Green’s functions satisfy

$$\begin{bmatrix} z - \epsilon_{\mathbf{k}} & \sigma M & \sigma \Delta_{\mathbf{k}} \\ \sigma M & z - \epsilon_{\tilde{\mathbf{k}}} & 0 \\ \sigma \Delta_{\mathbf{k}} & 0 & z + \epsilon_{-\mathbf{k}} \end{bmatrix} \begin{bmatrix} G_{\mathbf{k}\mathbf{k}}^{\sigma}(z) \\ G_{\tilde{\mathbf{k}}\tilde{\mathbf{k}}}^{\sigma}(z) \\ \bar{F}_{\mathbf{k}\mathbf{k}}^{\sigma}(z) \end{bmatrix} = \begin{bmatrix} 1 \\ 0 \\ 0 \end{bmatrix}, \quad (2)$$

where $\tilde{\mathbf{k}} = \mathbf{k} - \mathbf{Q}$, and where $G_{\mathbf{k}\mathbf{k}'}^{\sigma}(\omega)$ and $\bar{F}_{\mathbf{k}\mathbf{k}'}^{\sigma}(\omega)$ are Fourier transforms of the retarded and anomalous Green’s functions:

$$\begin{aligned} G_{\mathbf{k}\mathbf{k}'}^{\sigma}(t) &= -i \langle \{c_{\mathbf{k}\sigma}(t), c_{\mathbf{k}'\sigma}^{\dagger}(0)\} \rangle \Theta(t) \\ \bar{F}_{\mathbf{k}\mathbf{k}'}^{\sigma}(t) &= -i \langle \{c_{-\mathbf{k}\bar{\sigma}}^{\dagger}(t), c_{\mathbf{k}'\sigma}^{\dagger}(0)\} \rangle \Theta(t). \end{aligned}$$

The density of states $\rho(\omega) = -\frac{1}{\pi} \text{Im} \sum_{\mathbf{k}, \sigma} G_{\mathbf{k}\mathbf{k}}^{\sigma}(\omega + i0^+)$, plotted in Fig. 3(e)-(h), is determined by the poles of $G_{\mathbf{k}\mathbf{k}}^{\sigma}(\omega)$. For reference, a few constant-energy contours of the spectrum are shown in Fig. 4 for a case with $M = \Delta^{(d)} = 0.3$. The interested reader is directed to Ref. [45] for an extensive discussion of the normal state spectrum of this model. In the coexisting state, there

are two features of interest: first, at low energies the spectrum resembles that of the pure superconductor and, second, there is a new saddle-point singularity (at “A” in Fig. 4) which arises because of the coexisting order. In the limit $M \gg \Delta$, the origin of the saddle-point is fairly transparent: $G_{\mathbf{k}\mathbf{k}}^{\sigma}(z)$ has three poles corresponding to upper and lower magnetic bands with dispersion $E_{\pm} = (\epsilon_{\mathbf{k}} + \epsilon_{\tilde{\mathbf{k}}})/2 \pm [(\epsilon_{\mathbf{k}} - \epsilon_{\tilde{\mathbf{k}}})^2/4 + M^2]^{1/2}$ and a hole-band with dispersion $E_0 = -\epsilon_{\mathbf{k}}$. When $\Delta_{\mathbf{k}}$ is nonzero, there is an avoided crossing of E_0 and E_- which results in the saddle point. Both features of the dispersion are evident in $\rho(\omega)$ [Fig. 3(f)], which resembles the pure d -wave superconductor at low ω , and has a resonance at the saddle-point energy, $\omega = 0.38$. This model appears to capture several aspects of the inhomogeneous spectra in Fig. 3(a)-(d). First, it predicts the overall suppression of spectral weight on magnetic energy scales. Second, it predicts the occurrence of a subgap resonance. Third, it shows that while a d -wave-like tunneling gap survives to fairly large values of M , there is an inward shift in the position of the apparent “coherence peaks” as M increases. This is purely a band structure effect resulting from the reduction of spectral weight at the antinodal points, and has nothing to do with a reduction of $\Delta^{(d)}$. Fourth, it suggests that because AF nesting does little to disrupt the band structure near the nodal points, there will be a much smaller Fermi surface discontinuity for nodal quasiparticles crossing between SC and AF domains than for antinodal quasiparticles. This mechanism is one possible explanation for relative uniformity of the low energy spectrum measured in STM experiments when compared with the spectrum near the gap edge.

This model makes one other, somewhat subtle, prediction which appears to be relevant to the numerical work. Fig. 4 shows several constant energy contours for the middle and upper bands. For small M , the bottom of the upper band lies below the top of the middle band. As M is increased, however, a gap will appear in $\rho(\omega)$. Because the nesting points (the points at which $\epsilon_{\mathbf{k}} = \epsilon_{\mathbf{k}+\mathbf{Q}}$) lie near the antinodal points, the gap, when it opens, does so near the coherence peak energy, as in Fig. 3(g). [Notice that the energy at which the gap appears depends on both the band structure, and on $\Delta^{(d)}$. Hence, the gap in Fig. 3(g) appears at a higher energy than for a pure antiferromagnet. Furthermore, $\Delta^{(d)}$ tends to enhance the magnitude of the gap.] The key difference between Fig. 3 (b) and (c), where the coherence peaks evolve smoothly in the former and collapse in the latter, appears to be the presence of an AF gap in the spectrum. I remark that while there is a threshold value of M at which a gap forms, other kinds of order may not have such a threshold. For example, a charge density wave which nests between parallel antinodal sections of the Fermi surface may gap out the coherence peaks for any degree of ordering.

A second consequence of having a gap in $\rho(\omega)$ is that scattering resonances may produce exponentially localized bound states at energies within the energy gap. The

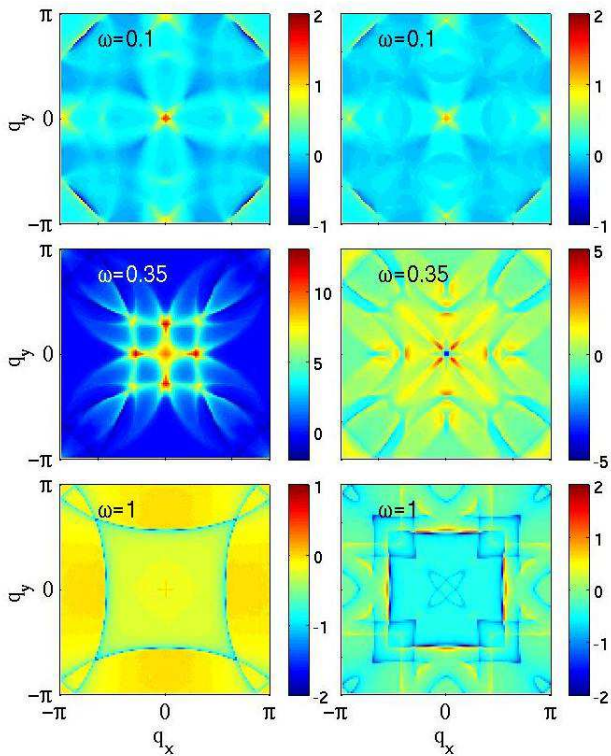


FIG. 5: Response kernel for disorder. The imaginary part of $\Lambda_3(\mathbf{q}, \omega)$ is shown for three values of ω for the coexisting order (left column) and pure superconducting (right column) cases. The parameters are the same as in Fig. 3(f) (left column) and (e) (right column). At low energy, the kernel is similar for both models (top row). The saddle point (labelled “A” in Fig. 4) causes the peak at $\mathbf{q} \approx (\pi/2, 0)$ to split into two at $\omega = 0.35$.

resonance at $\omega = 0.35$ in Fig. 3(c), for example, is very sharp, and localized to only the few sites nearest the core of the AF domain. Furthermore, its energy is close to where the spectral gap opens in the pure AF, making it a good candidate for the kind of local resonance discussed here. There are several sources of scattering—the inhomogeneity of the SC and AF order parameters, and the impurity Coulomb potential—which are not included in the homogeneous model, which could give rise to a bound state.

D. Weak charge modulations

Weak charge modulations have been observed in underdoped BSCCO,^{6,30} sparking an ongoing debate as to the extent to which spatial modulations of the LDOS can distinguish Friedel oscillations of quasiparticles from a tendency towards charge-ordering. In this section I will address two slightly different questions which arise from this debate. First, I will discuss charge ordering in the context of the current calculations. Second, I will

discuss the broader question of the extent to which a hidden order (an order which does not couple directly to the charge) can be revealed by quasiparticle scattering.

In Sec. II A, the self-consistent calculations show that a large charge inhomogeneity occurs in the hole-doped domains, and arises because of randomness in the impurity locations. In contrast, the undoped domains are remarkably homogeneous simply because they are free from impurities. The charge inhomogeneities are not particularly evident at energies near the Fermi level, but become apparent at large energies. The calculations do not find a local charge ordering, although the kind of weak modulations seen in Ref. [7] would be difficult to see on the finite-size lattices used in numerical calculations. Even if the current calculations do not admit charge ordering, it is likely that only minor modifications to Eq. (1) are needed to generate charge-ordered phases. By analogy with the self-consistent solutions for the AF phase, one would expect that these charge ordered phases would coexist with superconductivity throughout the system because of the proximity effect. This is in contrast to experiments in BSCCO,⁷ however, which see ordered charge modulations only in “pseudogap” domains. A resolution to this puzzle may be the fact that the charge distribution is uniform in underdoped domains, but is disordered in hole-doped domains. If the CDW order parameter is easily pinned by donor atoms, then it may also be locally suppressed by donor-related disorder.

The second question is whether hidden order can be revealed through the Fourier transformed density of states of a disordered superconductor. In order to get some sense of how disorder affects the LDOS, I return to the model of homogeneously coexisting order described in the previous section. I calculate the response kernel,^{32,34}

$$\Lambda_3(\mathbf{q}, \omega) = \sum_{\mathbf{k}} \text{Tr}_{\sigma} [G_{\mathbf{k}\mathbf{k}}^{\sigma}(\omega) G_{\mathbf{k}+\mathbf{q}\mathbf{k}+\mathbf{q}}^{\sigma}(\omega) - F_{\mathbf{k}\mathbf{k}}^{\sigma}(\omega) F_{\mathbf{k}+\mathbf{q}\mathbf{k}+\mathbf{q}}^{\sigma}(\omega)],$$

which describes the effects of scattering from impurities on the Fourier transformed density of states $\rho(\mathbf{q}, \omega)$. The results are shown in Fig. 5. At low ω , $\Lambda_3(\mathbf{q}, \omega)$ is similar for both coexisting order and for the pure d -wave superconductor while, at higher energies, the effects of antiferromagnetism become significant. At $\omega = 0.35$ (the energy of the saddle point marked “A” in Fig. 4) the pronounced resonances along the $(\pi, 0)$ and $(0, \pi)$ directions are split by the antiferromagnetism. One surprising result of these calculations is that $\Lambda_3(\mathbf{q}, \omega)$ differs significantly from the pure d -wave result even for energies much larger than M , suggesting that the effects of even weak ordering should be easily visible. At the same time, however, there is no obvious signature of the AF \mathbf{Q} -vector in the response kernel at most energies. In other words, AF ordering distorts the response kernel from the bare kernel, but does so in a nontrivial way. In particular, all features in $\Lambda_3(\mathbf{q}, \omega)$ disperse with ω . Thus, it appears that unless the nucleated order couples directly to the charge density, it will generally be difficult to distinguish

different kinds of order from the Fourier transformed density of states.

III. CONCLUSIONS

I have studied a mean-field extended Hubbard model in which charge is doped inhomogeneously because of randomness in the donor-atom positions. AF and SC order compete, and in the homogeneous case, are separated by a first order phase transition. Self-consistent calculations find that, because of inhomogeneity in the local doping, AF order coexists inhomogeneously with superconductivity. The AF moments spontaneously form π -shifted domain walls which are pinned to donor-atom sites. At low doping, the self-consistent solutions resemble pinned smectics, i.e. quasi-one-dimensional superconductors running along AF domain walls. Because of the proximity effect, both SC and AF correlations are actually present throughout the lattice. This picture appears to be consistent with neutron scattering studies in LSCO,⁴⁰ suggesting that AF and SC order coexist, and naturally explains the field-dependence of the AF moment, since any suppression of superconductivity by a magnetic field will enhance the AF moment.

At higher doping, the self-consistent calculations evolve towards a homogeneous d -wave superconductor interspersed with underdoped pockets with large AF moments. This latter “phase-separated” system superficially resembles the situation in BSCCO, although it is generally unclear whether the “pseudogap” domains in BSCCO have any kind of nucleated secondary phase. To address this question, I studied the local spectrum of a single, isolated AF pocket embedded in a homogeneous SC background. While no single calculated spectrum reproduces all details of the experimental measurements, several features such as the collapse of the coherence peaks, the occurrence of low-energy spectral features, and the relative homogeneity of the low energy spectrum, are broadly consistent with the kinds of spectra measured in, for example, Ref. [7]. Certain experimental aspects—notably the presence of weak nondispersing charge modulations—are not reproduced in my calculations. In general, the calculated spectra at low energies show a richer spectrum of peaks than is observed experimentally.

At this point, the effect of disorder on the spectrum of the isolated AF pocket is not understood. Earlier studies of point-like defects in d -wave superconductors show that this may not be a trivial effect. A single strong-scattering

point-like impurity introduces a sharp resonance near the Fermi level. As the disorder level increases, the resonances split, are inhomogeneously broadened, and evolve into an impurity band (see Ref. [46] for a recent summary). When the response of the SC order parameter to the disorder is included self-consistently, the SC gap tends to restore itself⁴⁷ by shifting spectral weight away from the Fermi level. Indeed, it is a general feature of interacting electrons in disordered media that the system can lower its energy by suppressing the density of states at the Fermi level. Further calculations, currently in progress, are needed to establish whether all the spectral features discussed in Sec. II B survive in the disordered limit.

Finally, although the calculations were performed for a model in which superconductivity and antiferromagnetism compete, I expect many of the findings to apply to other models of competing order. Three results, in particular, are expected to be general. First, when the domain sizes are small (as they appear to be in BSCCO), the proximity effect is extremely important, and has a significant impact on the local density of states. It was *never* found, in calculations, that the spectrum of the antiferromagnetic pocket resembles that of a bulk antiferromagnet. Rather, a better toy model appears to be one of coexisting homogeneous superconductivity and antiferromagnetism. Second, the gapping of the spectrum near the antinodal points by local ordering is a mean-field mechanism by which coherence peaks may be locally suppressed. Up to now, it has been generally understood that suppression of coherence peaks occurs through strong inelastic scattering at higher energies. For AF order, there is a threshold value of the magnetization for the gapping of the antinodal quasiparticles, but this may not be universal and other kinds of order (eg. CDW) may lead to suppression of coherence peaks for even small ordering. Finally, these calculations also suggest a natural reason that nodal quasiparticles should be less affected than antinodal quasiparticles by charge inhomogeneities, since the Fermi surface mismatch between domains is smallest for the nodal quasiparticles.

Acknowledgments

The author would like to acknowledge helpful conversations with P. J. Hirschfeld and R. J. Gooding. This work was supported in part by Research Corporation grant CC5543.

¹ T. Cren *et al.*, Phys. Rev. Lett. **84**, 147 (2000).

² S.-H. Pan *et al.*, *Nature* **413**, 282 (2001).

³ C. Howald, P. Fournier, and A. Kapitulnik, Phys. Rev. B **64**, 100504 (2001).

⁴ K.M. Lang, V. Madhavan, J. E. Hoffman, E. W. Hudson, H. Eisaki, S. Uchida and J.C. Davis, *Nature* **415**, 412 (2002).

⁵ C. Howald, H. Eisaki, N. Kaneko, A. Kapitulnik,

- cond-mat/0201546
- ⁶ C. Howald, H. Eisaki, N. Kaneko, M. Greven, A. Kapitulnik, Phys. Rev. B **67**, 014533 (2003).
 - ⁷ K. McElroy et al., cond-mat/0404005.
 - ⁸ F. C. Zhang, C. Gros, T. M. Rice, and H. Shiba, Supercond. Sci. Technol. **1** 1 46 (1988).
 - ⁹ Ziqiang Wang, Jan R. Engelbrecht, Shancai Wang, Hong Ding, Shugeng H. Pan, Phys. Rev. B **65** 064509 (2002).
 - ¹⁰ Arun Paramakanti, Mohit Randeria, and Nandini Trivedi, cond-mat/0305611; See also P. W. Anderson *et al*, cond-mat/0311467 and references therein.
 - ¹¹ D. Poilblanc and T. M. Rice, Phys. Rev. B **39**, 9749 (1989).
 - ¹² J. Zaanen and O. Gunnarsson, Phys. Rev. B **40**, 7391 (1989).
 - ¹³ H. J. Schultz, Phys. Rev. Lett **64**, 1445 (1990).
 - ¹⁴ M. Kato et al, J. Phys. Soc. Jpn. **59**, 1047 (1990).
 - ¹⁵ J. M. Tranquada et al, Nature **375**, 561 (1995); Phys. Rev. B **54**, 7489 (1996).
 - ¹⁶ Daniel Podolsky, Eugene Demler, Kedar Damle, and B. I. Halperin, Phys. Rev. B **67**, 094514 (2003).
 - ¹⁷ Matthias Vojta, Phys. Rev. B **66**, 104505 (2002).
 - ¹⁸ I. Affleck and J. B. Marston, Phys. Rev. B **37**, 8865 (1987).
 - ¹⁹ M. Vojta and S. Sachdev, Phys. Rev. Lett. **83**, 3916 (1999).
 - ²⁰ Shou-Cheng Zhang, Science **275**, 21 (1997).
 - ²¹ A. Polkovnikov, S. Sachdev, M. Vojta, and E. Demler, Int. J. Mod. Phys. B **16**, 3156 (2002).
 - ²² T. Pereg-Barnea and M. Franz, Phys. Rev. B **67**, 060503 (2003).
 - ²³ Gonzalo Alvarez, Matthias Mayr, Adriana Moreo, and Elbio Dagotto, cond-mat/0401474.
 - ²⁴ Han-Dong Chen, Oskar Vafek, Ali Yazdani, and Shou-Cheng Zhang, cond-mat/0402323.
 - ²⁵ Xiao-Gang Wen and Patrick A. Lee, Phys. Rev. Lett. **76** 503 (1996).
 - ²⁶ H. J. Schulz, Phys. Rev. B **39**, 2940 (1989).
 - ²⁷ C. Varma, Phys. Rev. Lett. **83** 3538 (1999).
 - ²⁸ Cristina Bena, Sudip Chakravarty, Jingping Hu, and Chetan Nayak, Phys. Rev. B **69**, 134517 (2004)
 - ²⁹ J. E. Hoffman *et al.*, Science **295**, 466 (2002).
 - ³⁰ McElroy et al. Nature **422**, 592 (2003).
 - ³¹ Qiang-Hua Wang and Dung-Hai Lee, Phys. Rev. B **67**, 020511 (2003).
 - ³² Lingyin Zhu, W. A. Atkinson, and P. J. Hirschfeld, Phys. Rev. B **69**, 060503 (2004).
 - ³³ Degang Zhang and C. S. Ting, Phys. Rev. B **67**, 100506 (2003)
 - ³⁴ L. Capriotti, D.J. Scalapino, and R. D. Sedgewick, Phys. Rev. B **68**, 014508 (2003).
 - ³⁵ T. Pereg-Barnea and M. Franz, Phys. Rev. B **68**, 180506 (2003)
 - ³⁶ M.-H. Julien et al, Phys. Rev. B **63**, 144508 (2001).
 - ³⁷ Y. Sidis et al, Phys. Rev. Lett. **86**, 4100 (2001).
 - ³⁸ H. A. Mook et al, Phys. Rev. B **66** 144513 (2002).
 - ³⁹ S. Sanna et al, cond-mat/0403608.
 - ⁴⁰ B. Lake *et al*, Nature **415**, 299 (2002).
 - ⁴¹ C. Panagopoulos, J. L. Tallon, B. D. Rainford, J. R. Cooper, C. A. Scott, and T. Xiang, Solid State Commun. **126**, 47 (2003).
 - ⁴² D. Raczkowski, A. Canning, and L. W. Wang, Phys. Rev. B **64**, 121101 (2001).
 - ⁴³ V. J. Emery, S. A. Kivelson, and J. M. Tranquada, Proc. Natl. Acad. Sci. **96**, 8814 (1999); S. A. Kivelson, E. Fradkin, and V. J. Emery, Nature **393**, 550 (1998).
 - ⁴⁴ See e.g. A. M. Martin and James F. Annett, Phys. Rev. B **57** 8709 (1998); Roger Haydock and Ronald L. Te, Phys. Rev. B **49**, 10845 (1994).
 - ⁴⁵ Andrey V. Chubukov and Dirk Morr, Physics Reports **288**, 355 (1997).
 - ⁴⁶ Lingyin Zhu, W. A. Atkinson, and P. J. Hirschfeld, Phys. Rev. B **67**, 094508 (2003).
 - ⁴⁷ W. A. Atkinson, P. J. Hirschfeld, and A. H. MacDonald, Phys. Rev. Lett. **85**, 3922 (2000).